Available online at www.sciencedirect.com
SCIENCE DIRECT®
Cement & Concrete Composites 27 (2005) 627–636
Cement & Concrete Composites
www.elsevier.com/locate/cemconcomp

Characterizing fiber dispersion in cement composites using AC-Impedance Spectroscopy

L.Y. Woo [a], S. Wansom [a], N. Ozyurt [b], B. Mu [b], S.P. Shah [b], T.O. Mason [a,*]

[a] Department of Materials Science and Engineering, Center for Advanced Cement-Based Materials, Northwestern University, 2220 North Campus Drive, Evanston, IL 60208-0001, USA

[b] Department of Civil Engineering, Center for Advanced Cement-Based Materials, Northwestern University, 2145 Sheridan Road, Evanston, IL 60208-0834, USA

Received 4 May 2004; accepted 16 June 2004

Abstract

A novel method is developed to evaluate fiber dispersion issues in short (or discontinuous) fiber-reinforced cement composites. Fiber orientation, global segregation (i.e., as a result of gravitational settling or improper mixing), and local aggregation (i.e., small fiber agglomerates distributed uniformly throughout the matrix) are quantified using an electrical measurement technique. The method is based on AC-Impedance Spectroscopy (AC-IS) and uses the intrinsic conductivity approach to characterize fiber dispersion through a process that is able to isolate some of the effects. A flow chart is developed to describe the method, which consists of 3D AC-IS measurements, a point probe technique, and a dispersion factor (DF) analysis.

Keywords: Fiber orientation; Fiber dispersion; Electrical impedance spectroscopy; Steel fiber composites

1. Introduction

The use of fiber reinforcement in cement-based composites has led to significant improvements in the mechanical properties of an otherwise brittle matrix, especially under tensile loads. Already used for various non- or semi-structural purposes, fiber-reinforced cement composites (FRCs) could be extended to more load-bearing applications as a result of the increase in ductility, toughness, and strength with the fiber addition [1]. To achieve this goal, a critical factor in determining the effectiveness of fibers in improving mechanical performance is fiber dispersion, which includes both how the fibers are oriented and their location and arrangement within the cement matrix.

Non-uniform fiber dispersion may severely limit the ability of the fibers to improve the composite properties [2–4]. In the case of oriented fibers, improvements in performance vary in different directions, which may or may not be desirable depending on the application. For fibers with random orientations but non-uniform distribution in the matrix, crack growth would be easier than in a matrix with uniform fiber dispersion. The easier crack growth results from the increase in fiber-free areas. Mechanical failure from cracking begins first with the formation of fine discontinuous microcracks throughout the matrix, which then coalesce to form larger cracks that eventually cause the material to fail. The main role of fibers in increasing the strength of the brittle matrix is in controlling the failure mechanisms by bridging the cracks and making crack formation and coalescence more difficult [5]. The fiber-free areas in poorly dispersed composites act as flaws where crack initiation and propagation occur more easily [6].

* Corresponding author. Tel.: +1 847 491 3198; fax: +1 847 491 7820.
E-mail address: t-mason@northwestern.edu (T.O. Mason).

0958-9465/$ - see front matter © 2004 Elsevier Ltd. All rights reserved.
doi:10.1016/j.cemconcomp.2004.06.003

In developing FRCs for structural applications, controlling and characterizing fiber dispersion is vital to maximizing the mechanical properties and performance. Established techniques to investigate fiber dispersion using image analysis [6–8] can be destructive and time consuming. An electrical measurement technique may alleviate these concerns. Extensive research has been conducted examining the electrical properties of FRCs either for electrical purposes (e.g., electromagnetic shielding and thermistors), but more often for monitoring strain and damage in the composites [9,10]. Chung [9,10] have investigated DC electrical properties of FRCs and attributed changes in resistance to microstructural changes such as fiber pull-out, fiber realignment, and/or changes in fiber spacing when the composite is under static or dynamic loading.

The effectiveness of AC electrical properties to investigate FRCs has also been demonstrated [11–15]. AC-Impedance Spectroscopy (AC-IS) of composites with conductive fibers (e.g., steel and carbon) results in a frequency-dependent behavior [15]. The response appears as a dual cusp in Nyquist plots (real vs. negative imaginary impedance). The dual-cusp behavior is caused by fibers behaving insulating at low frequencies (analogous to DC measurements) and conducting at high frequencies [13–15]. The change in behavior results from the existence of a high impedance interface on the conductive fibers, which shorts due to displacement currents through the interface at high frequencies. For example, in cement composites with steel fibers, the high impedance interface is an oxide that forms due to the high pH environment of the cement. Therefore, for composites with high impedance interfaces on the fibers, AC-IS provides additional information not available from DC measurements.

Previous work has resulted in the development of a universal equivalent circuit model to understand the "frequency-switchable" behavior [16]. The work demonstrates how AC-IS can be used to investigate fiber properties such as fiber loading and aspect ratio (length divided by diameter) in non-percolating systems (when the conductive fibers do not form a continuous path through the material, which would otherwise result in a dramatic change in resistance over a small fiber-loading range). In this work, electrical measurements with AC-IS are developed to monitor fiber dispersion in FRCs. The issues examined include fiber orientation, global segregation of fibers (e.g., settling of large fibers due to gravity), and local aggregation due to the formation of small fiber agglomerates distributed uniformly throughout the matrix.

2. Experimental procedures

Cement composite samples were produced with type I ordinary Portland cement (OPC) in cubic geometries (86 mm on a side) in polycarbonate molds. Samples were stored at 100% relative humidity, and electrical measurements were made at 7 days. The mixing procedures varied slightly for the experiments and are described in detail below.

The electrodes for the 2-point AC-IS measurements were achieved with a "wet" technique where large 0.5 mm thick steel plates were placed in reservoirs of 1 M NaCl solution or pressed against sponges soaked in 1 M NaCl solution that were then in intimate contact with both ends of the sample. Fig. 1 shows the experimental configuration. For both the reservoir and sponge methods, the bottom steel plate was approximately the size of the area of the sample (86 mm × 86 mm). For the reservoir method, the top steel plate was slightly smaller in order to fit inside the reservoir. The size of the steel plates did not affect the electrical measurements, which were dependent upon the electrolyte (1 M NaCl solution) making contact with the entire surface of the sample. Both the reservoir and sponge methods yielded similar resistance values. The steel plates at the

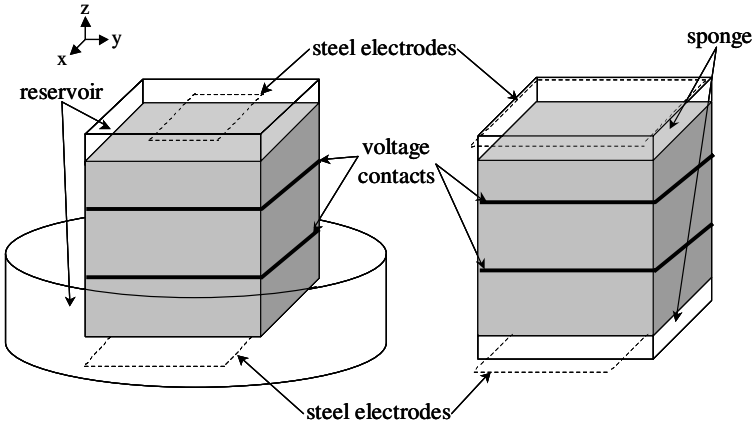

Fig. 1. Experimental setup for the 2-point AC-IS and 4-point DC measurements. See text for details.

end of the samples also served as the current leads for the 4-point DC measurements, with tightly wrapped 0.25 mm diameter steel wire loops at 1/4 and 3/4 positions along the sample (see Fig. 1) acting as the voltage contacts.

For the orientation experiments, 0.35 vol% large steel fibers (12 mm long, 0.5 mm diameter) were placed manually into the OPC matrix with a water-to-cement ratio (w/c) of 0.4 by weight. The use of larger fibers emphasized the orientation effect, and the small fiber loading was helpful in allowing the placement of individual fibers by hand. The cement powder and water were mixed by hand for 3 min before mixing at high speed in a commercial blender for 2 min to achieve homogeneity. The paste was then allowed to set for approximately 3 h to achieve a sufficiently high viscosity to allow the fibers to be arranged and remain in planar and uniaxial configurations without settling. For the random configuration, the fibers were mixed in by hand as opposed to being placed individually. AC-IS and DC measurements were made in all three directions.

To simulate the global segregation of fibers, 1 vol% steel fibers (6 mm long, 0.16 mm diameter; Bekaert, Belgium) were mixed randomly into the bottom third of the cubic sample leaving the top two-thirds of the sample fiber-free. The cement powder and fibers were dry mixed in a commercial blender for 1 min at low speed before adding the water. The composite paste was then mixed at low speed for another minute before pausing for 30 s to scrape the mixer and resuming at high speed for 2 min. The plain paste was mixed in a similar manner (without the addition of the fibers). The 7-day-old hardened sample was turned on its side and scanned across the top with a "point" probe electrode that consisted of a 6 mm diameter flat sponge disk saturated with 1 M NaCl solution, contacted above with a small steel plate electrode, and pressed against the sample. The counter electrode consisted of the usual large steel plate using the "wet" electrode technique, where a saturated sponge made contact with the entire bottom surface of the sample. Ten equally spaced AC-IS measurements were made across the top surface of the sample (see inset of Fig. 5).

In the local aggregation experiments, three different loadings (1, 2, and 4 vol%) of steel fibers (6 mm long, 0.16 mm diameter; Bekaert, Belgium) at two different w/c ratios (0.3 and 0.35) were examined to determine the effect, if any, of fiber loading and w/c ratio on the resulting fiber dispersion. The mixing routine followed that of the global segregation samples as outlined above. AC-IS and DC measurements were made in all three directions.

Two-point AC-IS measurements were made with a Solartron 1260 impedance/gain-phase analyzer using Z-60 personal computer software for data acquisition (Schlumberger, Houston, TX). The excitation voltage was set at 1 V, and the samples were scanned from 11 MHz to 0.1 Hz with data collected at 20 steps per frequency decade. In certain instances, to confirm the low-frequency cusp values and obviate external electrode contributions, 4-point DC measurements were made with a programmable current source and digital multimeter using LabVIEW personal computer software for data acquisition (Keithley, Models 220 and 2000, Cleveland, OH). The resistance values from DC measurements were geometry-corrected in order to compare them with the AC-IS derived values. Current was applied to the outer electrodes (1 mA increments from 10 to –10 mA) while measurements were made at the voltage contacts in the 4-point testing configuration, as seen in Fig. 1.

3. Results and discussion

3.1. The AC-IS and intrinsic conductivity approach

AC-IS involves the application of a low-amplitude AC excitation by surface electrodes over a range of frequencies and then measurement of the current response (i.e., gain and phase angle) by the impedance analyzer. Each frequency generates a single datum (current response) that has both real and imaginary components and can be shown in a Nyquist plot, which is negative imaginary impedance vs. real impedance. Fig. 2 shows data for samples used in the orientation study. Both samples (with and without fibers) show a partial arc to the right of the low-frequency (LF) cusp; the partial arc is associated with the external electrode response, not the composite. For the plain OPC sample, there is

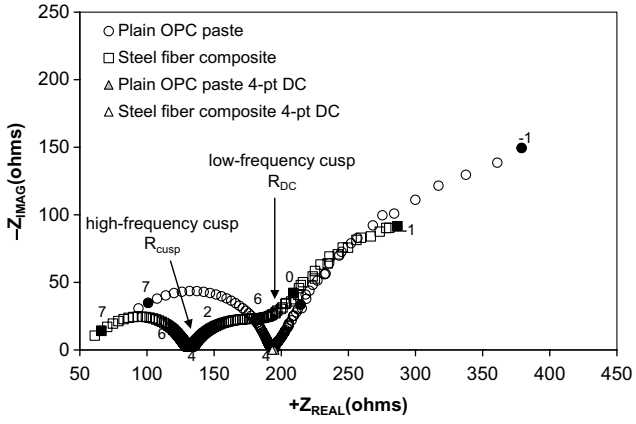

Fig. 2. Nyquist plot for data from orientation experiments, 0.35 vol% steel fibers (12 mm long, 0.5 mm diameter) placed manually in uniaxial arrangement (and measured in the direction of alignment) and plain OPC paste, both with 0.4 w/c at 7 days. The DC measurements are nearly identical and appear as discrete points (open and shaded triangles) on the *x*-axis. The numbers alongside darkened points and at the cusps are Log frequency (Hz) markers.

a single-bulk arc with a clearly discernable LF-cusp that corresponds to the measured DC resistance (the discrete point on the x-axis indicating only a real impedance contribution), confirming that the LF-cusp is analogous to the DC resistance.

The sample with fibers shows two bulk arcs with an additional high-frequency (HF) cusp. Unlike the plain OPC, the LF-cusp in the composite is more difficult to read since it does not reach the x-axis (real impedance value) due to its convolution with the external electrode response. The convolution is a result of the similarity in time constants between the oxide coating on the fibers and the oxide coating on the electrode. Nevertheless, the inflection point is discernable and corresponds well with the value of R_{DC} from 4-point DC. Therefore, DC measurements are not necessary to measure the LF-cusp.

The good agreement of the LF-cusp and DC resistances of the composite with those of the plain OPC sample indicates that the fibers behave as if insulating; their presence at low-volume fractions does not significantly alter the DC resistance. In the analysis of data for this work, the DC values were used due to good agreement with the LF-cusp values. The HF-cusp in the fiber sample is where the oxide coating shorts out so that the fibers behave conducting, and its value is at a lower resistance than R_{DC}. It should be stressed that only AC-IS is able to measure the value of the HF-cusp.

For composites with low-fiber loadings (i.e., in the dilute regime), an intrinsic conductivity approach can be used to understand the resulting electrical behavior in terms of the expected normalized conductivity, which is the composite conductivity (σ) divided by the matrix conductivity (σ_m). The method is based on each particle geometry having an "intrinsic conductivity", which is the first order coefficient in volume fraction (ϕ) in the following equation ([17]):

$$\frac{\sigma}{\sigma_m} = \frac{R_{DC}}{R_{cusp}} = 1 + [\sigma]_{\Delta}\phi; \quad \Delta = \frac{\sigma_f}{\sigma_m}, \tag{1}$$

where R_{DC} is the same as the LF-cusp, R_{cusp} is the HF-cusp, Δ is the ratio of the fiber conductivity (σ_f) to the matrix conductivity, and higher order terms of ϕ are neglected for low fiber loadings. The intrinsic conductivity, $[\sigma]$, is a function of Δ (written as a subscript in Eq. (1)) and of the geometry of the particle. For highly conductive particles, $\Delta \to \infty$, and for insulating particles, $\Delta \to 0$. The normalized conductivity is calculated from the two cusp values (LF and HF) in AC-IS measurements.

There are no simple analytical solutions for the intrinsic conductivity of conductive ($\Delta \to \infty$) thin right cylinders (i.e., fibers), but recent work has produced a modified form of the Fixman equation relating the intrinsic conductivity to the aspect ratio (AR), or length divided by diameter of the fibers [18]:

$$[\sigma]_{\infty} = \frac{1}{3}\left(\frac{2(AR)^2}{[3\ln\{4(AR)\} - 7]} + 4\right). \tag{2}$$

From the above relationship, as the AR of the conductive fiber increases, so does the value of the intrinsic conductivity, resulting in a dramatic increase in composite conductivity for a given volume fraction (e.g., at AR = 20, intrinsic conductivity is approximately 47, and at AR = 100, intrinsic conductivity is approximately 630). The higher the AR of the fiber, the more effectively it increases the composite conductivity at a given volume fraction. However, at low volume fractions, insulating fibers with aspect ratios greater than 10 have an intrinsic conductivity of approximately $-5/3$ that is independent of AR. Insulating fibers have a negligible influence on composite conductivity so that only the plain matrix is measured. Consequently, AC-IS will be relatively ineffective in detecting the presence of insulating (e.g., polymer) fibers, but in the case of conducting fibers, it allows the LF-cusp (i.e., when the conductive fibers behave insulating) to be used for normalization so that a separate measurement of the fiber-free matrix is not required. Therefore, the normalized conductivity, or composite conductivity divided by the matrix conductivity, can be calculated from a single AC-IS measurement of a composite sample with conducting inclusions [17,18].

The intrinsic conductivity of right cylinders, as calculated by the modified Fixman equation for a given AR, describes how the composite should behave electrically (as in Eq. (1)) for a given volume fraction, when the fibers are perfectly dispersed and randomly oriented. Knowing the AR and volume fraction, deviation from the expected behavior can be used to quantify fiber dispersion.

3.2. Orientation

Previous work with a model system consisting of a single conductive fiber has demonstrated the effectiveness of AC-IS in sensing alignment of fibers [14]. When the fiber axis was aligned with the applied field direction, the dual-cusp behavior was clearly evident. At the HF-cusp frequency, a large part of the matrix was bypassed by current flow via the conductive fiber. However, as the fiber was rotated away from the field direction, the HF-cusp began to approach the LF-cusp, resulting in single-cusp behavior once the fiber axis was perpendicular to the field direction. The similarity of the response for the perpendicular fiber to the field with that of the fiber-free matrix is due to the fact that only the thin fiber diameter acts as a short-circuit path for current flow at high frequencies, which is negligible. Consequently, more fibers aligned in the direction of the applied field will result in an increased HF-cusp conductivity as compared to randomly oriented fibers.

For the orientation samples used in this study, the placement of fibers by hand minimized global segregation (i.e., settling) and local aggregation (i.e., fibers agglomerating) effects in order to isolate the effect of alignment. Measurements were made in all three directions yielding an "effective" intrinsic conductivity in the x, y, and z directions as given below (from Eq. (1)):

$$[\sigma]_{\Delta(i)} = \frac{\left(\frac{R_{DC}}{R_{cusp}}\right)_i - 1}{\phi} = \frac{\left(\frac{\sigma}{\sigma_m}\right)_i - 1}{\phi}; \quad i = x, y, z. \tag{3}$$

The effective intrinsic conductivity in each direction is then normalized by the total sum of the intrinsic conductivities:

$$\Sigma = [\sigma]_{\Delta(x)} + [\sigma]_{\Delta(y)} + [\sigma]_{\Delta(z)} \tag{4}$$

The resulting fractional x, y, and z effective intrinsic conductivities for the uniaxial, planar, and random samples were plotted on a triangular diagram, as seen in Fig. 3. The center point (+) in Fig. 3 represents equal contributions from each direction or a perfectly random arrangement, with the dotted line showing how the data would shift for increasing planar (x–y plane) alignment, and the solid line showing how the data would shift for increasing uniaxial (along the x-axis) alignment. The open symbols for the random (triangle), planar (square), and uniaxial (circle) alignments are shown for the measured composites and agree reasonably well with the expected behavior. The measured data do not exactly match the expected behavior owing to the difficulty in producing perfectly random or aligned fiber samples. AC-IS is able to detect even slight off-axis or out-of-plane tilting of the fibers. Complementing the AC-IS work with other orientation characterization techniques such as digitized micrographs of cross-sections and/or 3D computed X-ray tomography will be the subject of future work.

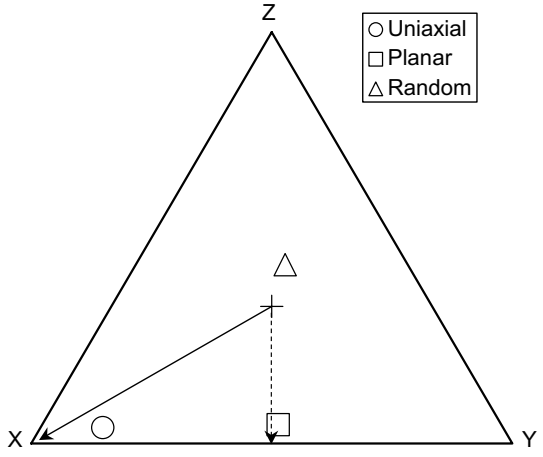

Fig. 3. Triangular diagram showing the fractional contributions of each direction to the intrinsic conductivity, which correlates with the amount of fibers aligned in that direction. The dotted arrow indicates how data would shift for increasing planar (x–y plane) alignment, and the solid arrow indicates how data would shift for increasing uniaxial (x-axis) alignment. The open symbols represent data from actual fiber composites (0.35 vol% steel fibers—12 mm long, 0.5 mm diameter—0.4 w/c at 7 days) in random (triangle), planar (square), and uniaxial (circle) arrangements.

Table 1
Average values of normalized conductivity ($\sigma/\sigma_{m,average}$) from the orientation experiments, from which intrinsic conductivities ($[\sigma]_{\infty,average}$) have been calculated demonstrating good agreement with the theoretical value from the Fixman Eq. (2)

	$\sigma/\sigma_{m,average}$	$[\sigma]_{\infty,average}$
Uniaxial	1.19 ± 0.11	54
Planar	1.20 ± 0.11	58
Random	1.14 ± 0.11	40
Theoretical	1.22	58.7

If there is neither measurable global segregation (see below) nor local aggregation, the average of the three effective intrinsic conductivities should match the modified Fixman equation (Eq. (2)) for a randomly oriented sample. Table 1 shows the average values of normalized conductivity ($\sigma/\sigma_{m,average}$) from the orientation experiments, from which average intrinsic conductivities have been calculated. For the uniaxial and planar arrangements, the intrinsic conductivity values are in excellent agreement with the value of 58.7 calculated from Eq. (2), corresponding to true random orientation. The slightly larger deviation from the theoretical value for the "random" specimen may be attributable to unintentional aggregation of the fibers (see below) from being mixed in by hand as opposed to manual placement. The averaged value of normalized conductivity for the random specimen, however, still matches the theoretical value within error. Therefore, the average of the AC-IS measurement in three directions provides a single overall sample parameter correcting for orientation effects and can be subsequently examined for other fiber dispersion issues.

3.3. Global segregation

Global segregation, which may arise from gravitational settling or improper mixing, is difficult to measure with the area electrodes used in the 3D AC-IS orientation experiments described above. Except in the most severe cases (when all the fibers are in one section of the sample) and only for a series arrangement (see Fig. A.1a), where the current travels sequentially through fiber-free areas and fiber-rich areas, does a detectable change in electrical properties occur. In a parallel arrangement (see Fig. A.1b), where the current goes through fiber-free areas and fiber-rich areas simultaneously, AC-IS measures the same response as for a

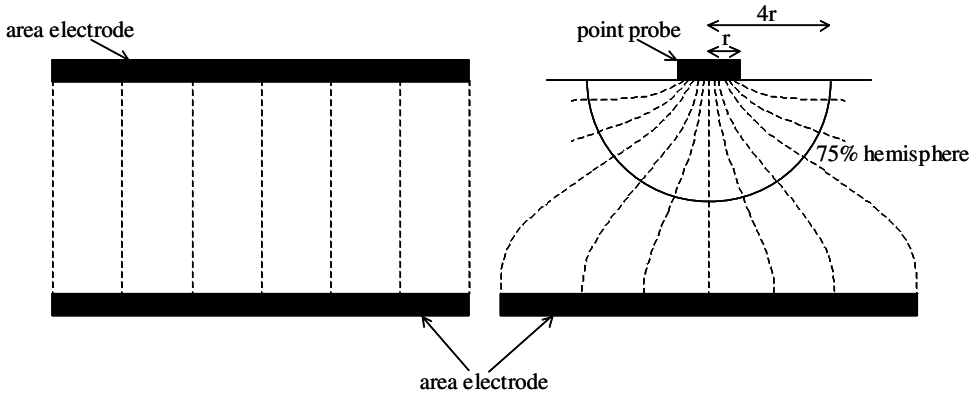

Fig. 4. Schematic of area electrodes vs. the point probe electrode with counter electrode. The spreading resistance is shown for a point electrode of circular geometry, which acts as a probe where 75% of the resistance occurs within a hemisphere that has a radius four times that of the probe radius.

sample with uniformly dispersed fibers. As a result, the global AC-IS response of a sample with segregation measured with area electrodes can be inconclusive. Appendix A provides more details on the series and parallel arrangements in global segregation.

The AC-IS "point" probe (described in Section 2) is necessary to investigate global segregation, which is associated with fiber-loading gradients due to areas of lower and higher fiber loading in the sample. Fig. 4 shows a schematic comparing the area electrode configuration with the point probe configuration, where the dashed lines show current flow. Based on a technique used in electroceramics to evaluate the electrical properties of grains vs. grain boundaries [19], the point probe measures the electrical properties in a small hemisphere located around the probe to explore changes in fiber loading as the probe is scanned along the surface of a sample.

As current bunches into or spreads out of a small electrode, an additional contribution to the measured resistance arises, known as the spreading resistance. The spreading resistance for a planar electrode with circular geometry is given by the Newman equation [20]:

$$R_{\text{spreading}} = \frac{1}{4\sigma r}, \tag{5}$$

where r is the radius of the electrode, and σ is the conductivity of the sample in the hemisphere being measured. This measured spreading resistance can be much higher than the overall bulk resistance of the sample. Fleig and Maier [21] reported that 75% of the spreading resistance occurs within a hemisphere that has a radius four times that of the contact radius, as shown in Fig. 4. Therefore, the point probe measures the electrical properties of the sample inside this hemisphere, whose volume is determined by the size of the probe.

There are two main issues in using the AC-IS point probe. The first issue addresses the relative contributions of the probe spreading resistance vs. the bulk resistance of the specimen. When the spreading resistance of the probe is much larger than the bulk resistance, the AC-IS measurement only reflects the electrical properties of the hemisphere being sampled or "probed", which is desirable to investigate global segregation. It is important to have a large counter electrode so that its spreading resistance is negligible compared to that of the probe. Decreasing the size of the probe will increase its spreading resistance, but the size of the hemisphere being sampled will also decrease. The second issue addresses how small the hemisphere can be and still provide meaningful information about fiber loading. The size of the point probe should be large enough so that the resulting hemisphere diameter is at least several times the fiber length, and the fiber loading should be sufficient to ensure that the probe hemisphere samples a significant number of fibers. For a sample with 1 vol% of 6 mm long, 0.16 mm diameter fibers examined with a 6 mm diameter probe, a 24 mm diameter hemisphere should have approximately 300 fibers if they are uniformly distributed throughout the matrix.

Due to the restrictions on the size of the probe in relation to the fibers, the AC-IS point probe may not give an absolute value for the fiber loading in the hemisphere because there would still be a bulk contribution to the measurement. Instead, the probe measures the extent of change in fiber loading across the sample. A constant resistance would indicate no global segregation, whereas a gradient would indicate where areas of higher and lower fiber loading occur.

For the sample in this study with fibers in one-third of the volume, ten AC-IS measurements were made, and the normalized conductivities were calculated from the HF- and LF-cusp resistances. From Eq. (1), the normalized conductivity is directly related to the volume fraction, or fiber loading in a sample. Fig. 5 shows the measured normalized conductivities as the AC-IS probe

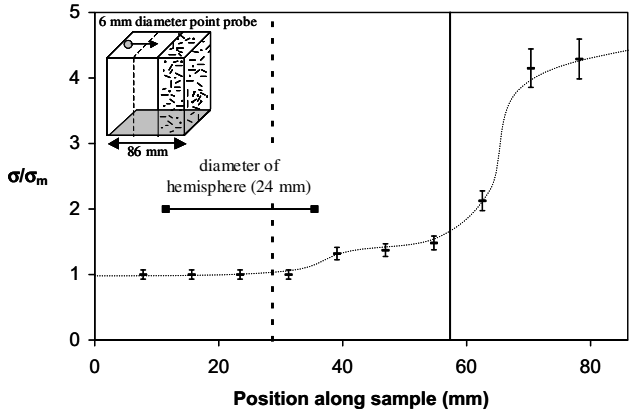

Fig. 5. Measured normalized-conductivity (fiber-loading) profile for a sample with fibers segregated to one end. The dashed and solid lines in the inset diagram correspond to the lines in the profile. The dotted line drawn through the data points serves to guide the eye. The diameter of the hemisphere is also shown for comparison. See text for details.

was stepped across the sample from the fiber-free to the fiber-rich end, with the size of the area being probed by the 6 mm diameter electrode shown for comparison (diameter of hemisphere being probed is 24 mm). At the fiber-free end, there was single-cusp AC-IS behavior resulting in a constant normalized conductivity of unity. However, as the probe began to sense the presence of fibers in the fiber-rich end, there was an increase in normalized conductivity, indicating an increase in fiber loading.

The measured interface between the fiber-free and fiber-rich region was not sharp, due to the size of the probe (and resulting hemisphere being probed) and the size of the fibers. A sharper interface or higher resolution result would be anticipated for a smaller probe, which would then require a sample with smaller fibers in order to register properties averaged over many fibers. The probe size has no upper limit, but resolution is sacrificed with increasing size, whereas the lower limit is dictated by the size of the fibers and ability of the probe to measure an average fiber loading in the small hemisphere being examined.

3.4. Local aggregation

Specimens with no detectable global segregation of fibers (by point probe analysis) can still exhibit local aggregation, e.g., due to fiber clumping uniformly distributed throughout the matrix, which is frequently found for composites with small fibers. Recently, we developed an AC-IS based "dispersion factor" (DF) analysis to establish the tendency for fiber clumping. The approach compares the response of a composite system without clumping [16]:

$$\frac{\sigma}{\sigma_m} = \frac{R_{DC}}{R_{cusp}} = 1 + [\sigma]_{\Delta}\phi, \tag{6}$$

to a composite system with clumping:

$$\frac{\sigma}{\sigma_m} = \frac{R_{DC}}{R_{cusp}} = 1 + [\sigma]_{\Delta}\phi' + \sum [\sigma]_{\Delta j}\phi_j, \tag{7}$$

where ϕ is the overall fiber volume fraction, ϕ' is the volume fraction of randomly dispersed fibers of intrinsic conductivity $[\sigma]_{\Delta}$, and ϕ_j is the volume fraction of the jth fiber "clump" of effective intrinsic conductivity $[\sigma]_{\Delta j}$. By subtracting 1 from both sides of Eqs. (6) and (7), and dividing Eq. (7) by Eq. (6), we arrive at the dispersion factor:

$$DF = \left[\frac{\left(\frac{\sigma}{\sigma_m}\right)_{measured} - 1}{\left(\frac{\sigma}{\sigma_m}\right)_{theory} - 1}\right] = \frac{\phi'}{\phi} + \frac{\sum [\sigma]_{\Delta j}\phi_j}{[\sigma]_{\Delta}\phi} \tag{8}$$

It should be stressed that $(\sigma/\sigma_m)_{theory}$ is taken from Eq. (6) based upon the fiber volume fraction and $[\sigma]_{\Delta}$ for the AR of the fibers (as per the modified Fixman Eq. (2)). The first term on the right side of Eq. (8) is the fraction of well-dispersed fibers, which defines the extent of local aggregation in the sample, and the second term is the contribution to the composite conductivity from poorly dispersed fibers or fiber clumps. Although the contribution from poorly dispersed fibers is smaller than that from the well-dispersed fibers, the second term is non-zero, depending on the exact nature of how the fibers are agglomerating. Therefore, the DF is only an upper limit for the percentage of well-dispersed fibers. However, for a perfectly dispersed composite with no fiber clumping, the second term must go to zero, and DF = 1, so that a DF near unity indicates good dispersion or negligible fiber agglomeration.

Experimentally, the $(\sigma/\sigma_m)_{measured}$ term is the average of (σ/σ_m) measured in the x, y, and z directions from 3D AC-IS measurements. This should eliminate any complications due to preferred alignment of fibers. Fig. 6 shows the DF results for varying volume fractions and w/c ratios from the local aggregation experiments. The

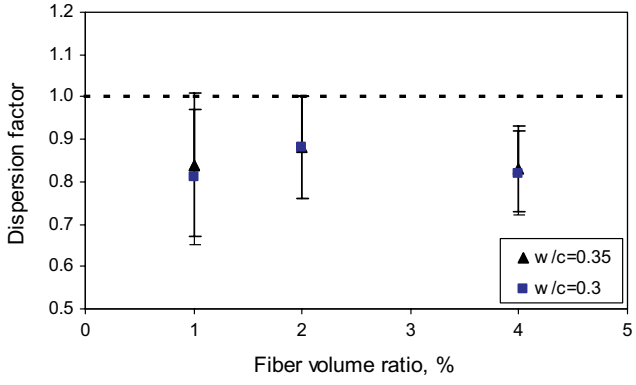

Fig. 6. Dispersion factor (DF) vs. volume fraction results for FRCs with steel fibers (6 mm long, 0.16 mm diameter) at 7 days for varying w/c ratios. The DF for a perfectly dispersed system is 1.0.

measured DFs were between 0.81 and 0.88, and the w/c ratio (0.3 and 0.35) did not seem to affect the DFs. However, the decreased DF from unity in every case indicates some level of agglomeration and a tendency for fiber clumping in the samples.

4. Conclusions

Electrical measurements using AC-Impedance Spectroscopy (AC-IS) are non-destructive and effective in characterizing the orientation and arrangement of conductive fibers in FRCs. The AC-IS method makes use of the intrinsic conductivity approach, which dictates how the conductivity of the composite should behave for fibers of a known aspect ratio (AR) and volume fraction in a randomly aligned and well-dispersed FRC. The deviation from theoretical behavior serves as the basis for quantifying fiber dispersion. Three fiber dispersion issues can be examined, including preferred orientation, global segregation (e.g., gravitational settling of fibers), and local aggregation (i.e., small fiber agglomerates uniformly distributed throughout the matrix).

3-D AC-IS measurements of samples result in directional effective intrinsic conductivities that can be shown in a triangle plot representing the fractional x, y, and z contributions to the overall intrinsic conductivity. The increased fractional contribution in a certain direction indicates that more fibers are aligned in that direction. The occurrence of global segregation is difficult to detect with large area electrodes; however, the AC-IS point probe allows the investigation of small regions in the composite (within a hemisphere determined by the size of the point probe) for fiber-loading gradients. A composite that has no fiber-loading gradients may still contain fiber agglomerates or clumps distributed uniformly throughout the matrix. The average of 3D AC-IS measurements can be used for local aggregation analysis, since this corrects for any orientation effects. A dispersion factor (DF) derived from the theoretical and measured behavior (averaged 3D AC-IS values) provides an upper limit for how well the fibers are dispersed. A value of unity indicates a perfectly dispersed sample, whereas values less than unity indicate some tendency for clumping depending on the nature of the fiber agglomeration.

Fig. 7 outlines the AC-IS approach for characterizing fiber dispersion. The AC-IS point probe is used to detect any global segregation due to settling or improper mixing of the sample. If there is global segregation, the gradient in fiber loading, as indicated by σ/σ_m, provides information about how the fibers are arranged. If there is no global segregation, the averaged 3D AC-IS value is used in a dispersion factor (DF) analysis, which quantifies local aggregation. The 3D AC-IS measurements indicate how fibers are oriented in the specimen. The approach can be extended to investigate fresh paste composites as well [22]. The use of AC-IS in monitoring fresh paste composites during processing is the subject of ongoing work.

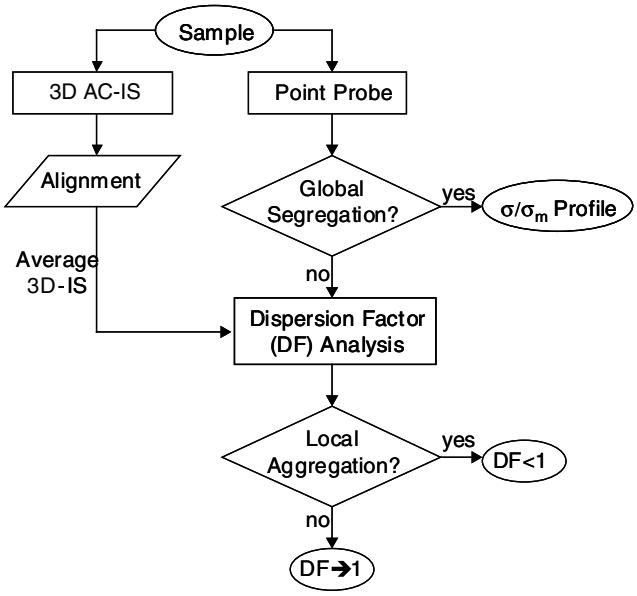

Fig. 7. Flow diagram detailing the AC-IS approach developed to investigate fiber dispersion issues in FRCs, which include orientation, global segregation (e.g., gravitational settling), and local aggregation (i.e., small fiber agglomerates uniformly distributed throughout the matrix).

Acknowledgments

The authors gratefully acknowledge the assistance of Edward J. Garboczi of the National Institute of Standards and Technology, Materials and Construction Research Division. This work was supported in part by the National Science Foundation under grant no. DMR-00-73197.

Appendix A

Two simplified AC-IS configurations can be considered in using large area electrodes to detect global segregation. Fig. A.1a shows the series arrangement when the conductive fibers are in layers perpendicular to the applied field direction. Fig. A.1b shows the parallel arrangement when the fibers are in layers parallel to the applied field direction. The overall measured conductivity (σ) divided by the matrix conductivity (σ_m) for both arrangements is related to the number of layers (L) with equal thickness, the volume fraction of each layer (where ϕ_i is the volume fraction of fibers in the ith layer), and the intrinsic conductivity of the conduct-

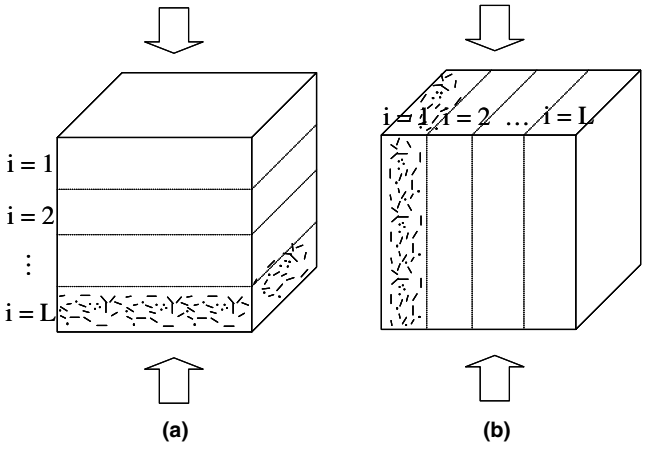

Fig. A.1. (a) In the series arrangement, fibers are settled in layers perpendicular to the applied field direction (block arrows). (b) In the parallel arrangement, fibers are settled in layers parallel to the applied field direction. Eqs. (A.1) and (A.2) (see Appendix A) describe the normalized conductivity for the two cases with reference to the volume fraction in each layer (ϕ_i) of identical thickness and the total number of layers (L).

ing fibers ($[\sigma]_\infty$) when the total volume fraction (ϕ_T) of the sample is known.

For the series arrangement (Fig. A.1a), the following expression describes the expected normalized conductivity:

$$\left(\frac{\sigma}{\sigma_m}\right)_{\text{series}} = \frac{L}{\left[\sum_{i=1}^{L} \frac{1}{(1+[\sigma]_\infty \phi_i)}\right]} \tag{A.1}$$

and for the parallel arrangement (Fig. A.1b):

$$\left(\frac{\sigma}{\sigma_m}\right)_{\text{parallel}} = \frac{\sum_{i=1}^{L}(1+[\sigma]_\infty \phi_i)}{L} = 1 + [\sigma]_\infty \sum_{i=1}^{L} \frac{\phi_i}{L} = 1 + [\sigma]_\infty \phi_T. \tag{A.2}$$

For the parallel arrangement, the normalized conductivity will not change for any amount of segregation, as demonstrated in Eq. (A.2). In the series arrangement, only dramatic amounts of global segregation cause a significant enough change in the normalized conductivity to indicate segregation. There is approximately ±10% error in normalized conductivity due to experimental error from sample dimension variations. Using Eqs. (A.1) and (A.2), Table A.1 shows theoretical values of normalized conductivity as measured by area electrodes for a bilayer sample (1 vol% fibers—6 mm long, 0.16 mm diameter, AR = 37.5, $[\sigma]_\infty = 118$) with small (25%) and dramatic (50%) amounts of depletion in one layer while keeping the total sample at 1 vol%. No change in normalized conductivity occurs for the parallel arrangement in either case as predicted by Eq. (A.2), and about a 10% change (very similar to the amount expected for experimental error) occurs for the series arrangement when one layer is half depleted of fibers. Significant conductivity change only occurs for the series arrangement when one layer is completely depleted. AC-IS with area electrodes is completely ineffective in measuring global segregation for the parallel configuration (when fibers are arranged in layers parallel to the applied field direction) and is somewhat effective, but only for dramatic amounts of segregation, in the series configuration (when fibers are arranged in layers perpendicular to the applied field direction).

Table A.1
Calculated values of normalized conductivity (σ/σ_m) using Eqs. (A.1) and (A.2) for bilayer samples with 1 vol% of 6 mm long and 0.16 mm diameter (AR = 37.5) fibers with different amounts depleted from one layer for both the series and parallel arrangements (see Fig. A.1)

Depletion in layer (%)	$(\sigma/\sigma_m)_{\text{series}}$	$(\sigma/\sigma_m)_{\text{parallel}}$
25	2.14	2.18
50	2.02	2.18
100	1.54	2.18
None	2.18	2.18

The value for no depletion, or a sample with uniformly dispersed fibers, is shown for comparison.

References

[1] Balaguru PN, Shah SP. Fiber-reinforced cement composites. USA: McGraw-Hill, Inc., 1992.
[2] Bentur A. Fiber-reinforced cementitious materials. In: Skalny JP, editor. Materials Science of Concrete. The American Ceramic Society; 1989. p. 223–85.
[3] Mobasher B, Stang H, Shah SP. Microcracking in fiber reinforced concrete. Cem Concr Res 1990;20:665–76.
[4] Banthia N, Bindiganavile V, Mindess S. Impact resistance of fiber reinforced concrete: A progress report. In: Proceedings, RILEM 4th International Workshop on High Performance Fiber Reinforced Cement Composites (HPFRCC4), Ann Arbor, USA, June 15–18, 2003. p. 117–31.
[5] Shah SP. Do fibers increase the tensile strength of cement-based matrices? ACI Mater J 1991;88:6.
[6] Akkaya Y, Picka J, Shah SP. Spatial distribution of aligned short fibers in cement composites. J Mater Civ Eng 2000;12:272–9.
[7] Chermant JL, Chermant L, Coster M, Dequiedet AS, Redon C. Some fields of applications of automatic image analysis in civil engineering. Cem Concr Compos 2001;23:157–69.
[8] Lawler JS, Wilhelm T, Zampini D, Shah SP. Fracture processes of hybrid fiber-reinforced mortar. Mater Struct 2003;37:197–208.
[9] Chung DDL. Composite materials for electronic functions. Switzerland: Trans Tech Publications; 2000.
[10] Chung DDL. Applied materials science: applications of engineering materials in structural, electronics, thermal, and other industries. Boca Raton, FL: CRC Press; 2001.
[11] Gu P, Xu Z, Xie P, Beaudoin JJ. An AC impedance spectroscopy study of micro-cracking in cement-based composites during compressive loading. Cem Concr Res 1993;23:675–82.
[12] Ford SJ, Shane JD, Mason TO. Assignment of features in impedance spectra of the cement-paste/steel system. Cem Concr Res 1998;28(12):1737–51.

[13] Torrents JM, Mason TO, Garboczi EJ. Impedance spectra of fiber-reinforced cement-based composites. Cem Concr Res 2000;30:585–92.
[14] Torrents JM, Mason TO, Peled A, Shah SP, Garboczi EJ. Analysis of the impedance spectra of short conductive fiber-reinforced composites. J Mater Sci 2001;36:4003–12.
[15] Mason TO, Campo MA, Hixson AD, Woo LY. Impedance spectroscopy of fiber-reinforced cement composites. Cem Concr Compos 2002;24:457–65.
[16] Woo LY, Wansom S, Hixson AD, Campo MA, Mason TO. A universal equivalent circuit model for the impedance response of composites. J Mater Sci 2003;38:2265–70.
[17] Douglas JF, Garboczi EJ. Intrinsic viscosity and the polarizabilities of particles having a wide range of shapes. In: Prigogine I, Rice SA, editors. Advances in chemical physics, vol. XCI. John Wiley & Sons; 1995.
[18] Hixson AD, Woo LY, Campo MA, Mason TO, Garboczi EJ. Intrinsic conductivity of short conductive fibers in composites by impedance spectroscopy. J Electroceram 2001;7:189–95.
[19] Fleig J, Maier J. Finite element calculations of impedance effects at point contacts. Electrochim Acta 1996;42:1003–9.
[20] Newman J. Resistance for flow of current to a disk. J Electrochem Soc 1966;113:501–2.
[21] Fleig J, Maier J. Surface conductivity measurements on AgCl single crystals using microelectrodes. Ber Bunsen-Ges Phys Chem 1996;100:607–15.
[22] Ozyurt N, Woo LY, Mu B, Shah SP, Mason TO. Detection of fiber dispersion in fresh and hardened cement composites. In: Workshop on Improving the Performance of Concrete Through Science and Engineering, Electronic Proceedings of the March 2004 meeting (Evanston, IL), RILEM Publications, Bagneux, France. 2004.